Supplement of Biogeosciences, 23, 3965–3980, 2026
https://doi.org/10.5194/bg-23-3965-2026-supplement

Biogeosciences Open Access EGU

Supplement of

Surface area and Ω-aragonite oversaturation as controls of the runaway precipitation process in ocean alkalinity enhancement

Niels Suitner et al.

Correspondence to: Niels Suitner (niels.suitner@uni-hamburg.de) and Jens Hartmann (geo@hattes.de)

Supplement

Overview experimental setups:

Gran Canaria (Taliarte, Spain - 27.988°N 15.367°W)

(adapted from Hartmann et al., 2023)

Oligotrophic coastal seawater ($TA_{initial}$ ~2411 ± 5 µmol kg^{-1}, DIC ~2006 ± 16 µmol kg^{-1}, pH ~8.15 ± 0.02, $\Omega_{aragonite}$ 4.4 ± 0.3, Sal. ~36.6 Temp. ~23 °C) was taken at 4 m depth in the vicinity of the harbor of Taliarte on the16th of September 2021. Nine batch solutions were prepared adding TA in nine steps of 300 µmol kg^{-1}, starting at an initial alkalinity value of ~2400 µmol kg^{-1} (fresh untreated seawater, ΔTA_0), with a maximum final treatment of TA_{final} ~4800 µmol kg^{-1} (ΔTA_{2400}). The TA enhancement was achieved by adding volumes of 0.5M NaOH stock solution. After taking an initial sample (day 0) from every batch, the remaining solutions were filled in portions of ~525 g into 500mL Dickson, each for a duration of 24 or 96 h. All bottles were stored airtight in the dark, at a temperature of ~24°C. For sampling each treatment was filtered through a 0.2µm filter to stop possible further reactions on larger particles and remove the biomass from the biotic approaches for further analysis. While filtering, all systems were kept airtight as much as possible to prevent gas exchange with the atmosphere. Samples were measured for TA, pH, salinity, conductivity, and temperature. TA was determined by titration with 0.02 M hydrochloric acid using an 888 Titrando autosampler (Metrohm). Calibration of TA and DIC measurements was determined against certified reference materials (CRM batches 143 and 190), supplied by Andrew Dickson, Scripps Institution of Oceanography (USA). To analyze for pH, salinity, conductivity, and temperature a WTW multimeter (MultiLine® Multi 3630 IDS, pH-probe: SenTix 940 pH-electrode, conductivity: TetraCon 925 cell, Xylem) was employed. The pH-probe was calibrated with WTW buffer solutions according to NIST/PTB in four steps (1.679–9.180 at 25 °C) and corrected for seawater after Badocco et al. (2021). For the TetraCon 925 cell 0.01 mol L^{-1} KCl calibration standards for conductivity cells (WTW, traceable to NIST/PTB) were used.

Raunefjorden (Bergen, Norway - 60.27° N, 5.20° E)

(adapted from Suitner et al., 2024)

Four sets of experiments were conducted between May and July 2022 using natural seawater from Raunefjorden (60.27° N, 5.20° E), close to the Espeland marine biological station (Bergen, Norway). All four experiments used the same setup. Firstly, 250 mL polystyrene cell culture bottles were filled with filtered seawater in a flow-through incubation box (PMMA) and incubated outdoors to follow the local light conditions. The box was covered in blue foil (172 Lagoon Blue Foil, LEE Filters, Burbank, CA, United States) to mimic the light conditions in the fjord at a depth of ~ 5 m. The temperature was regulated by recirculating fjord water in the incubation box, thus ensuring that the incubation temperature matched that of the fjord. To prevent the occurrence of substantial headspace throughout the experiment, each treatment level was divided into three to four separate bottles. The division allowed progressive volume removal during sampling while reducing the potential for gas exchange processes. Within each experiment, a new set of bottles was opened sequentially after three to four samplings. Alkalinity was enhanced using a 0.5 M NaOH (sodium hydroxide) stock solution for the non-CO_2-equilibrated treatments and a combination of $NaHCO_3$ (sodium bicarbonate, 0.4 M) and Na_2CO_3 (sodium carbonate, 0.2 M)

stock solutions for the preparation of the CO_2-equilibrated treatments. The latter were adjusted to attain equilibrium with the surrounding air's CO_2 concentration (~420 µatm). For each of the two, the experimental setups encompassed (1) abiotic conditions, achieved by removing organisms via filtration through a 0.2 µm filter, and (2) biotic conditions, where only the small phytoplankton community was included by using a 50 µm filter mesh to remove larger particles and organisms. The categorization into abiotic and biotic treatments aimed to determine the potential influences of biological activity or naturally occurring sediments, while also preserving the comparability of the experimental setup described in Hartmann et al. (2023). The experiments were conducted over a span of 2 months, with each incubation run for 20 or 25 d. The experiments were therefore partially separated in time, resulting in slight variations in starting conditions and average temperatures, ranging from 10 to 16 °C. Biotic and abiotic treatments were simultaneously conducted within each equilibration mode. The initial carbonate chemistry parameters of the collected seawater before manipulation were relatively constant for all approaches ($TA_{initial}$ ~2190 ± 10 µmol kg^{-1}, DIC ~1890 ± 20 µmol kg^{-1}, pH ~8.25 ± 0.05, $\Omega_{aragonite}$ 2.8 ± 0.4 and Sal. ~32.6 ± 0.1).

For carbonate chemistry analysis, 40–50 mL of incubated water was taken per sampling day and treatment level. Using a peristaltic pump connected to a 0.2 µm syringe filter, samples were filtered immediately to stop further reactions, remove particles, and prepare each sample for measurements. All treatments were measured without replicates for TA, pH, temperature, and salinity. Methods and devices for measuring TA, pH, temperature, and salinity were identical to experiments in Hartmann et al. (2023) – see above.

Outliers:

(adapted from Suitner et al., 2024)

Each TA treatment level (Raunefjorden, Bergen) was divided into three individual bottles. These bottles were sampled at defined time intervals. For the filtered CO_2-equilibrated experiment a complete set of bottles (sampling days 6 and 8), exhibited stable parameters at the same level throughout the experiment. In contrast, the set with the related sampling days 10, 15, and 20, continued the process of runaway precipitation uniformly. A similar phenomenon was observed in the filtered non-CO_2-equilibrated experiment. Again, bottles sampled on days 8, and 10 exhibited no significant changes, while bottles sampled on days 15, 20, and 25 showed continued precipitation. Despite thorough examination and multiple repetitive measurements on-site, no explanation for this behavior could be determined. The temporal alignment of both incidents (occurring between June 24 and June 28, 2022) suggests that an environmental factor, such as water temperature, sunlight intensity, or a specific aspect of the sampling procedure might have affected related bottles. Errors during the measurements were excluded by numerous iterations with check standards. Furthermore, the simultaneous impact on pH and TA indicates that the measured values were accurate.

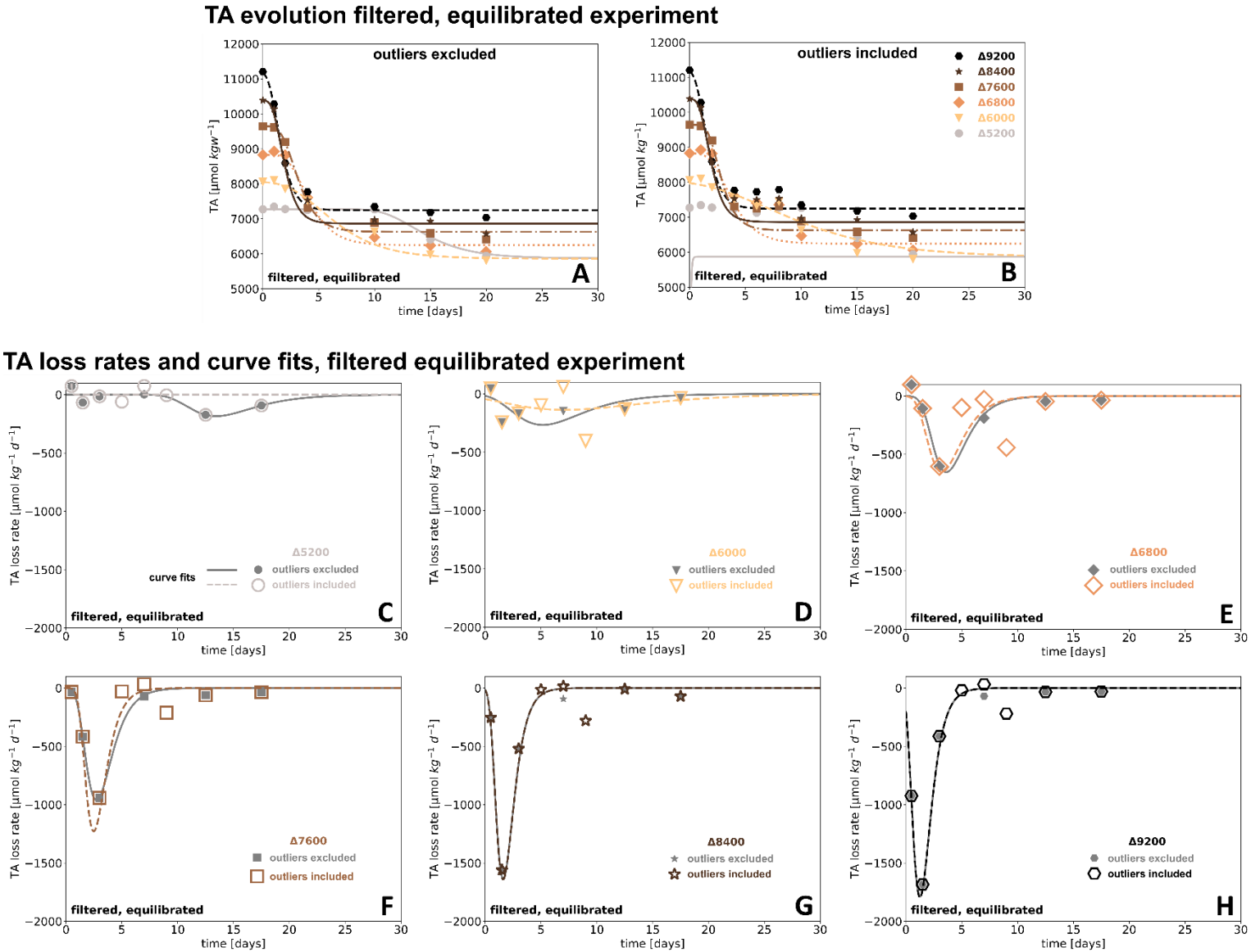

Figure S1: Comparison of TA evolution, TA loss rates, and corresponding curve fits with and without outliers, in the filtered equilibrated treatments. TA evolution excluding outliers (A) and including outliers (B). (C-H) TA loss rates and curve fits for each treatment level entering an accelerated precipitation phase, solid gray markers and lines: without outliers, hollow markers and dashed lines: outliers included. Curve fits differ in case outliers appear to fall into the accelerate precipitation phase of a treatment level, excluding the outliers was met by averaging the rate between the last and first measurement point before and after the period with outliers (days 6 and 8)

71

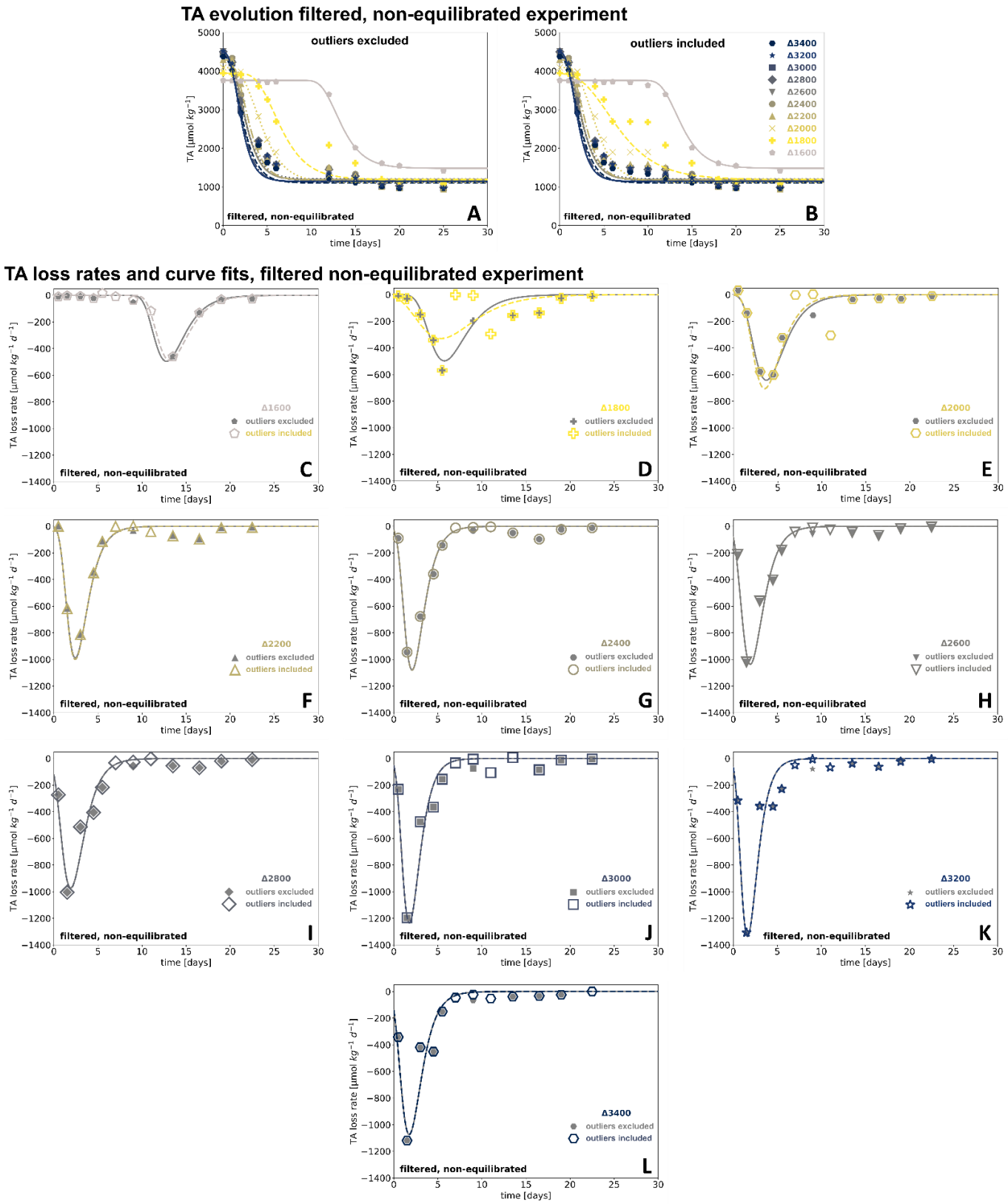

Figure S2: Comparison of TA evolution, TA loss rates, and corresponding curve fits with and without outliers, in the filtered non-equilibrated treatments. TA evolution excluding outliers (A) and including outliers (B). (C-L) TA loss rates and curve fits for each treatment level entering an accelerated precipitation phase, solid markers and lines: without outliers, hollow markers and dashed lines: outliers included.

72

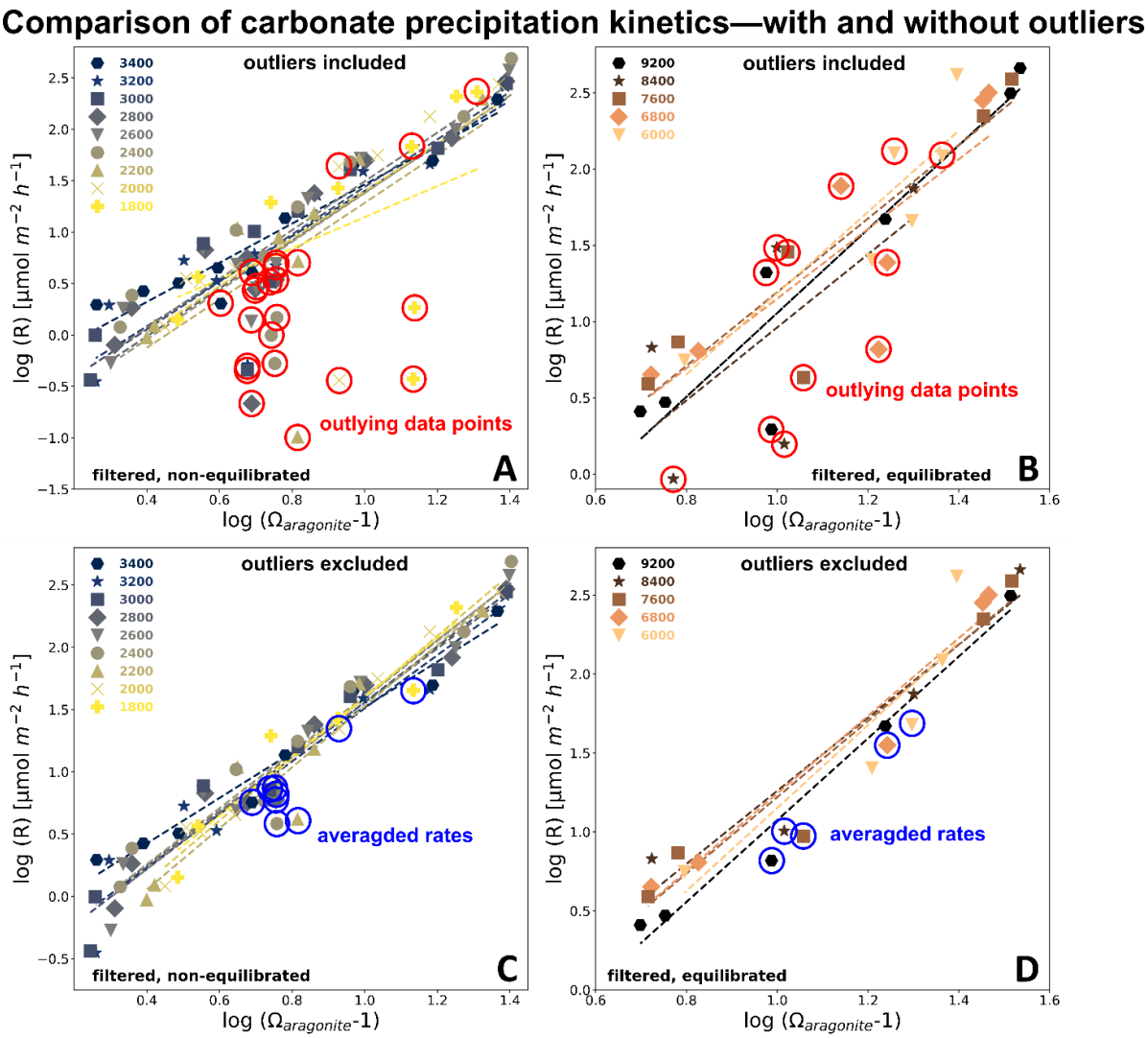

Figure S3: Comparison of carbonate precipitation kinetics for filtered treatments that entered the APP; (A) filtered neq with outliers, (B) filtered eq with outliers, (C) filtered neq without outliers, (D) filtered eq without outliers, red outlined data points: excluded outliers, note that some outliers exhibited an increase in TA during the precipitation process and could therefore not be plotted on a logarithmic scale; blue outlined data points: rates representing the average rate calculated between the last and first datapoint before and after the precipitation halted.

73

Table S1: Overview of the rate equation for the filtered neq approach, comparing scenarios with and without outliers. Also see Fig. S3.

Treatment $\log(R) = n(\Omega_{ar} - 1) + \log(k)$

	Outliers excluded			Outliers included		
ΔTA	n	log(k)	R^2	n	log(k)	R^2
3400	1.82	-0.30	0.963	1.90	-0.44	0.908
3200	2.13	-0.62	0.929	2.20	-0.79	0.788
3000	2.24	-0.68	0.955	2.31	-0.87	0.793
2800	2.18	-0.62	0.959	2.33	-0.95	0.707
2600	2.29	-0.70	0.952	2.37	-0.88	0.871
2400	2.25	-0.64	0.924	2.37	-0.99	0.658
2200	2.45	-0.93	0.906	2.35	-1.06	0.459
2000	2.47	-0.88	0.984	2.31	-0.91	0.575
1800	2.38	-0.78	0.924	1.51	-0.36	0.214

Table S2: Overview of the rate equation for the filtered eq approach, comparing scenarios with and without outliers. Also see Fig. S3.

Treatment $\log(R) = n(\Omega_{ar} - 1) + \log(k)$

	Outliers excluded			Outliers included		
ΔTA	n	log(k)	R^2	n	log(k)	R^2
9200	2.59	-1.52	0.823	2.60	-1.56	0.825
8400	2.31	-1.05	0.963	2.81	-1.80	0.718
7600	2.41	-1.19	0.942	2.41	-1.22	0.842
6800	2.46	-1.22	0.925	2.28	-1.13	0.690
6000	2.63	-1.47	0.977	2.66	-1.48	0.799

Table S3: Overview of coefficients for unfiltered neq treatments, also see Fig. 3 for the related numerical curve fits and Tab. S8 for cross-comparison of all treatments.

Treatment $f(t) = a\, e^{-be^{-ct}} + d$

ΔTA	**a**	**b**	**c**	**d**	**R^2**
2800	-3162.94	5.88	0.64	4426.60	0.97
2600	-3184.57	6.66	0.66	4458.90	0.94
2400	-3162.95	5.09	0.65	4466.20	0.99
2200	-3091.21	5.22	0.38	4292.50	0.96
2000	-2841.46	24.49	0.40	4106.00	0.98
1800	-2503.10	86.03	0.35	3924.60	0.99
1600	-1932.75	-252.65	-0.30	3686.50	1.00

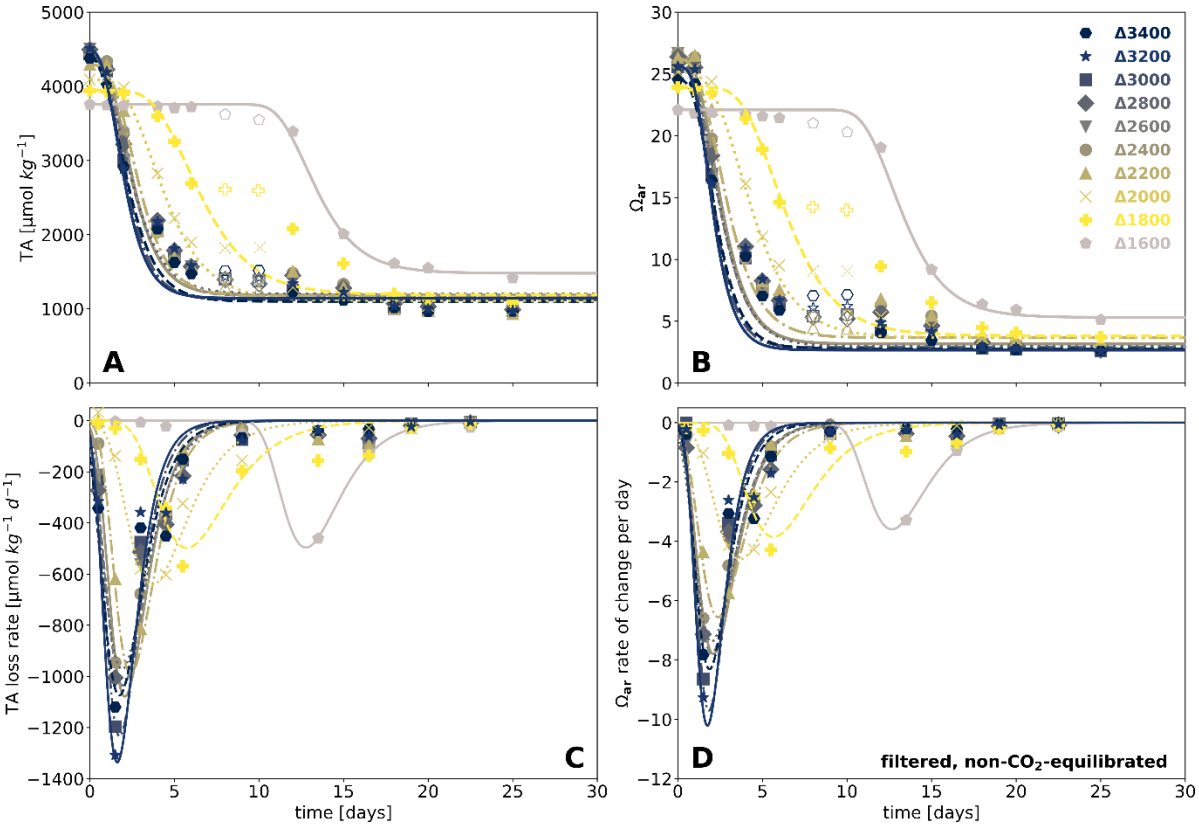

Figure S4: Results of the numerical curve fits – for the filtered neq approach, TA evolution over time (A), Ω_{ar} evolution over time (B), TA-loss rate over time (C), Ω_{ar} rate of change over time (D) Line plots: curve-fitted continuous functions, markers: measured data points, hollow markers: excluded datapoints, see chapter on outliers above, also see Tab. S4 for the determined coefficients of the curve fit.

Table S4: Overview of the coefficients for the filtered neq treatments curve fits, also see Fig. S4 and Tab. S8.

Treatment $f(t) = a\, e^{-be^{-ct}} + d$

ΔTA	a	b	c	d	R^2
3400	-3359.0	4.55	0.87	4460.4	0.86
3200	-3368.1	5.76	1.08	4511.3	0.87
3000	-3312.2	5.94	1.01	4437.7	0.90
2800	-3294.8	4.59	0.80	4497.5	0.90
2600	-3333.5	5.17	0.84	4506.1	0.91
2400	-3238.0	6.51	0.91	4426.4	0.94
2200	-3121.7	8.06	0.86	4294.1	0.96
2000	-2976.7	8.75	0.59	4090.1	0.95
1800	-2753.5	16.77	0.49	3943.1	0.89

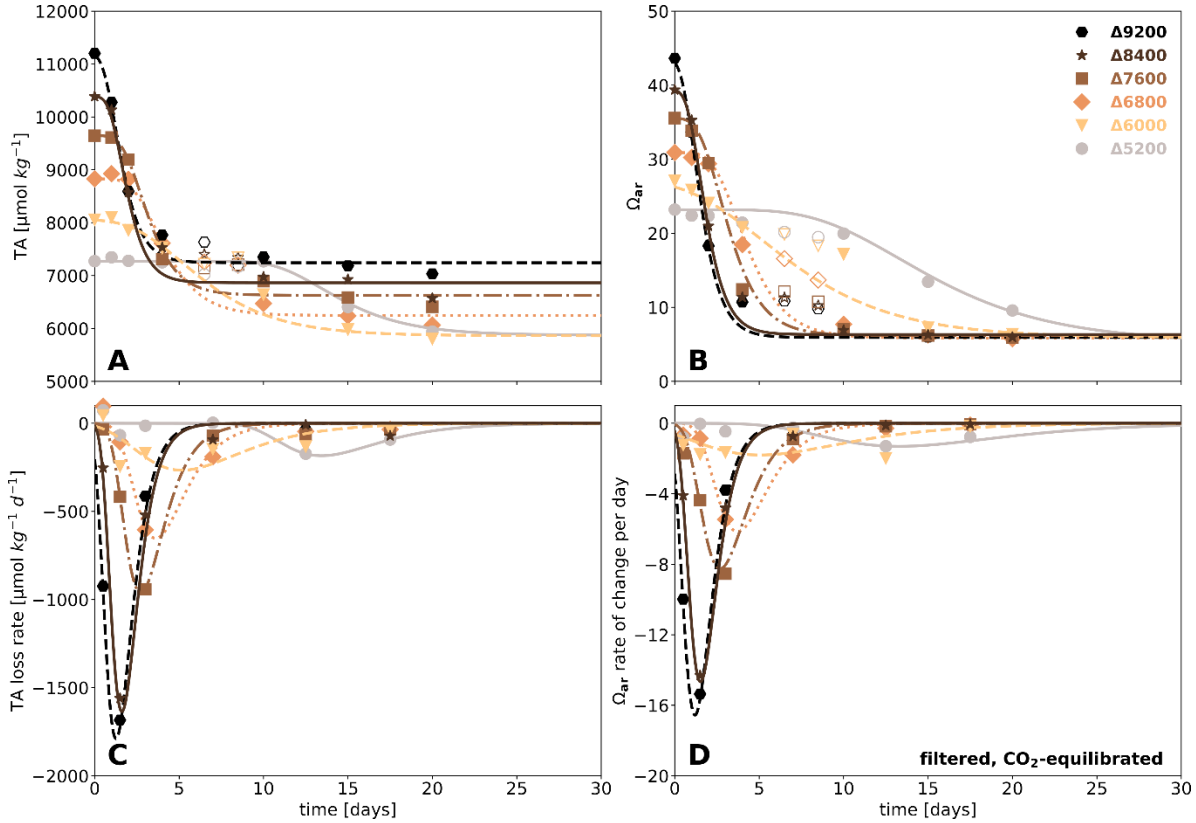

Figure S5: Results of the numerical curve fits – for the filtered eq approach, TA evolution over time (A), Ω_{ar} evolution over time (B), TA-loss rate over time (C), Ω_{ar} rate of change over time (D). Line plots: curve-fitted continuous functions, markers: measured data points, hollow markers: excluded datapoints, see chapter on outliers above, also see Tab. S5 for the determined coefficients of the curve fit.

Table S5: Overview of the coefficients for the filtered eq treatments curve fits, also see Fig. S5 and Tab. S8.

Treatment $f(t) = a\, e^{-be^{-ct}} + d$

ΔTA	a	b	c	d	R^2
9200	-3957.4	4.73	1.23	11202.3	0.99
8400	-3522.1	7.65	1.26	10387.4	0.98
7600	-3017.7	10.63	0.87	9646.6	1.00
6800	-2583.1	11.99	0.69	8829.9	0.99
6000	-2499.5	5.50	0.33	8058.7	0.70
5200	-1401.0	121.95	0.36	7273.7	0.99

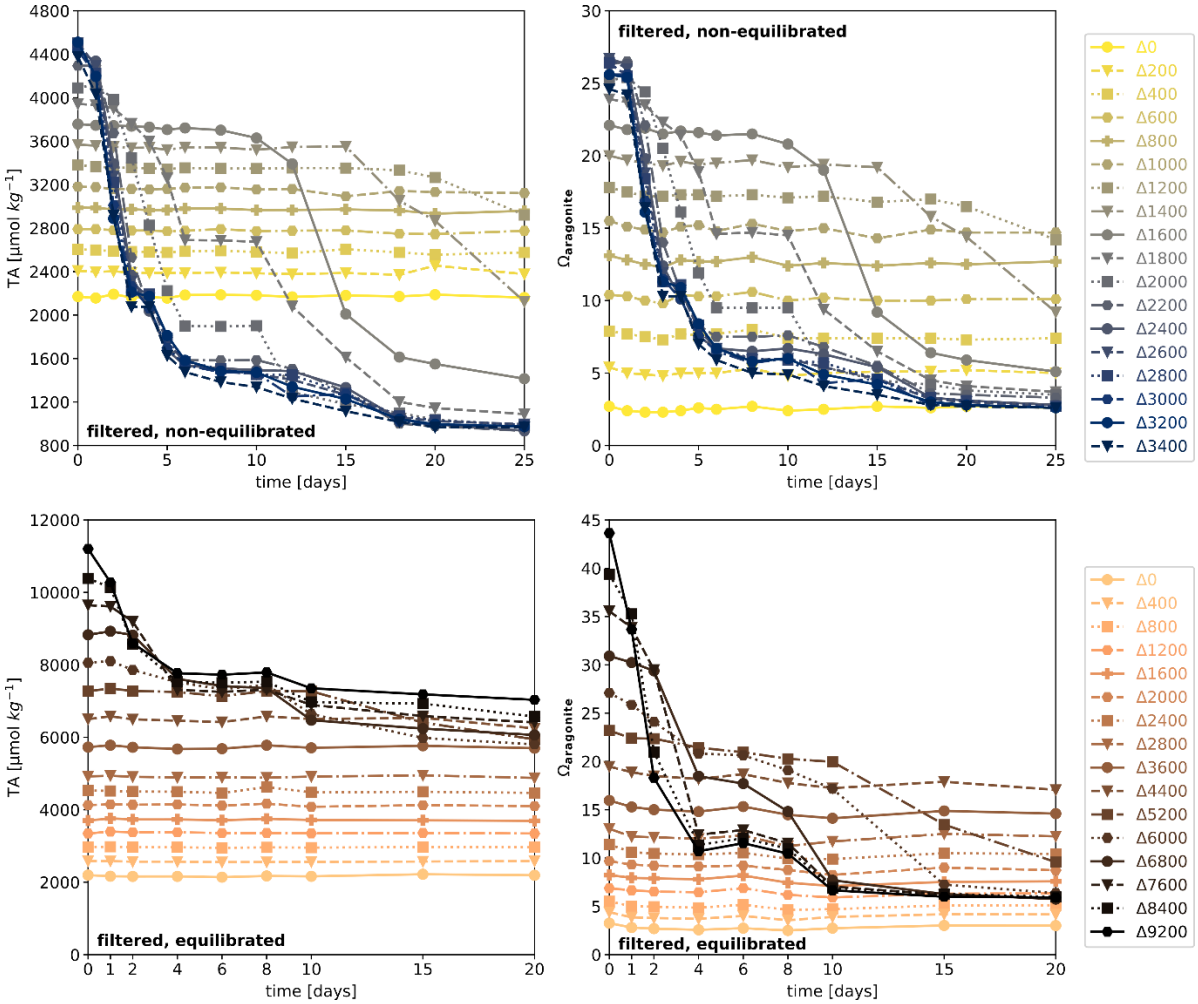

Figure S6: TA and Ω_{ar} raw data of the filtered treatment for cross comparison. See Suitner et al. (2024) for further details.

93

*Figure S7: Regressions describing the relationships between the coefficient **(b)** and the modeled induction time [A], as well as the coefficient **(c)** and the modeled APP timespan [B] for each approach. The shown regressions allow for the conversion of specifiable time-dependent characteristics of a runaway process to the coefficients of the presented inverse logistic function (Eq. (1)). Specified relationships should not be generalized and are only valid within the given conditions of each approach.*

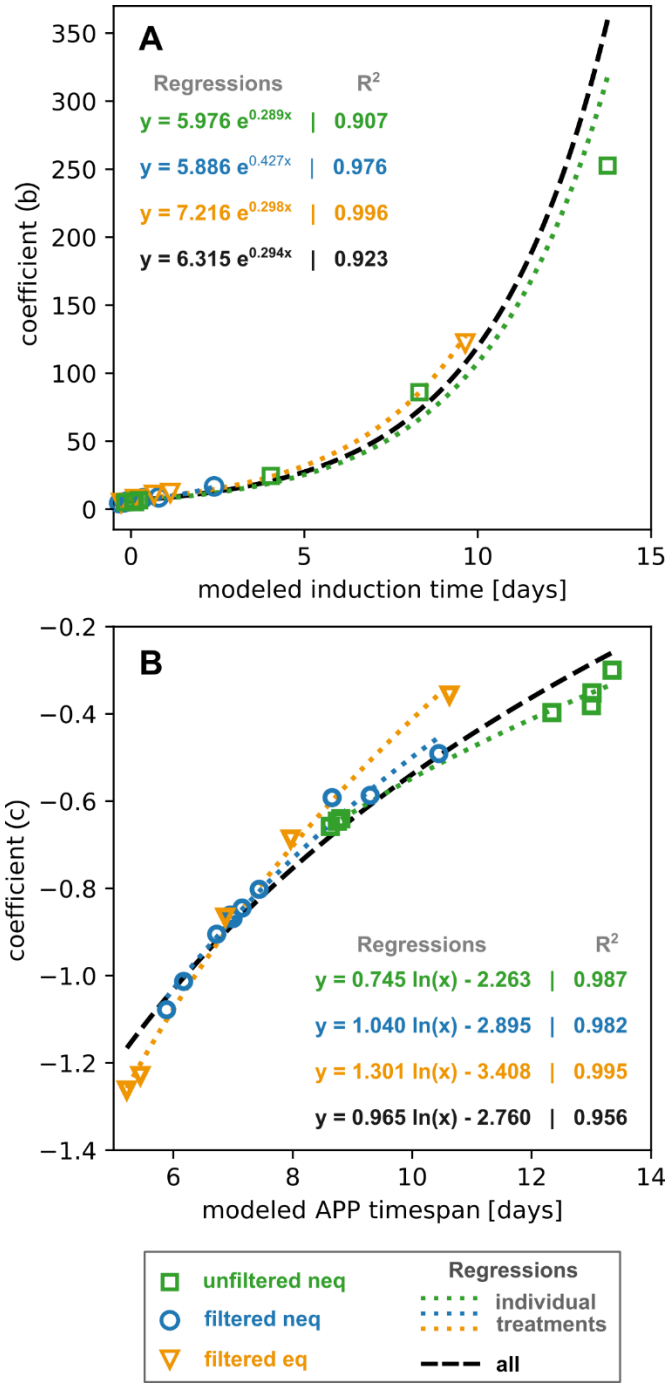

94

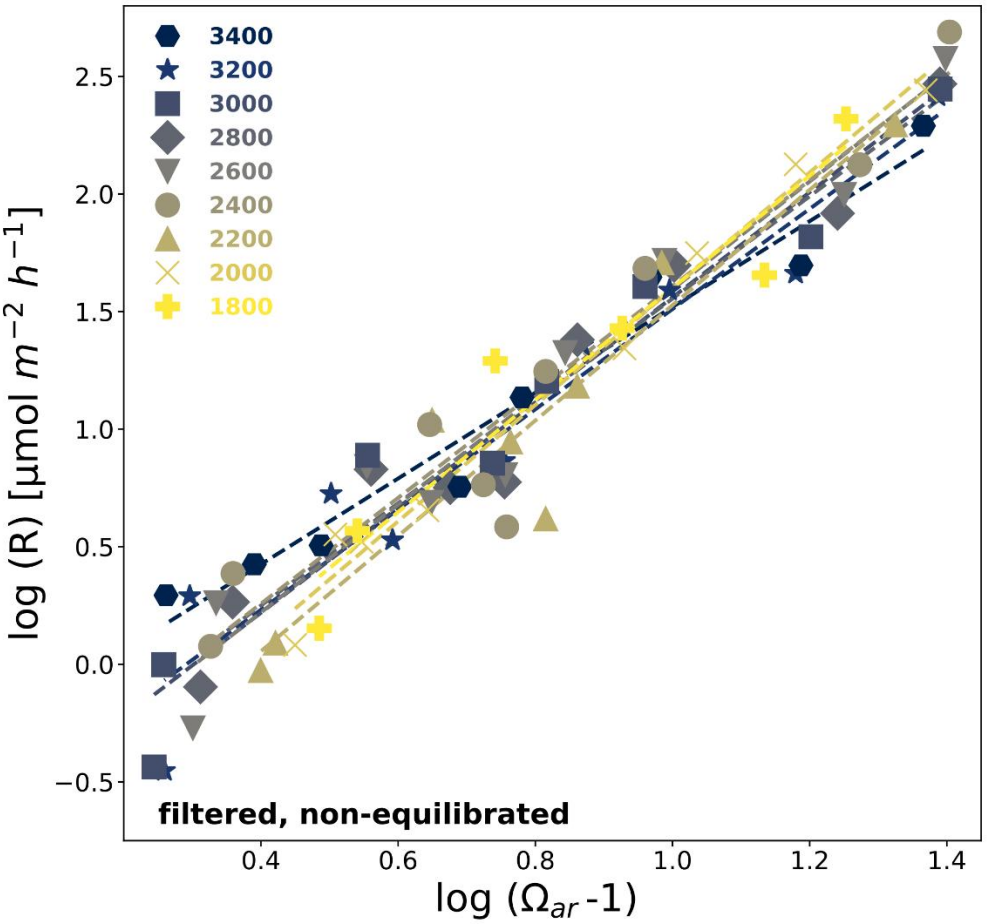

Figure S8: Carbonate precipitation kinetics for filtered neq treatments that entered the APP; see Tab. S6 for the related regressions and rate equations.

Table S6: Overview of coefficients and regressions of empirical rate equations for filtered neq treatments, also see Fig. S8 and Tab. S8.

Treatment $\log(R) = n(\Omega_{ar} - 1) + \log(k)$

ΔTA	n	log(k)	R^2	$\hat{\sigma}$
3400	1.82	-0.30	0.963	0.080
3200	2.13	-0.62	0.929	0.110
3000	2.24	-0.68	0.955	0.095
2800	2.18	-0.62	0.959	0.080
2600	2.29	-0.70	0.952	0.089
2400	2.25	-0.64	0.924	0.107
2200	2.45	-0.93	0.906	0.100
2000	2.47	-0.88	0.984	0.047
1800	2.38	-0.78	0.924	0.097
all	2.22	-0.66	0.937	0.201

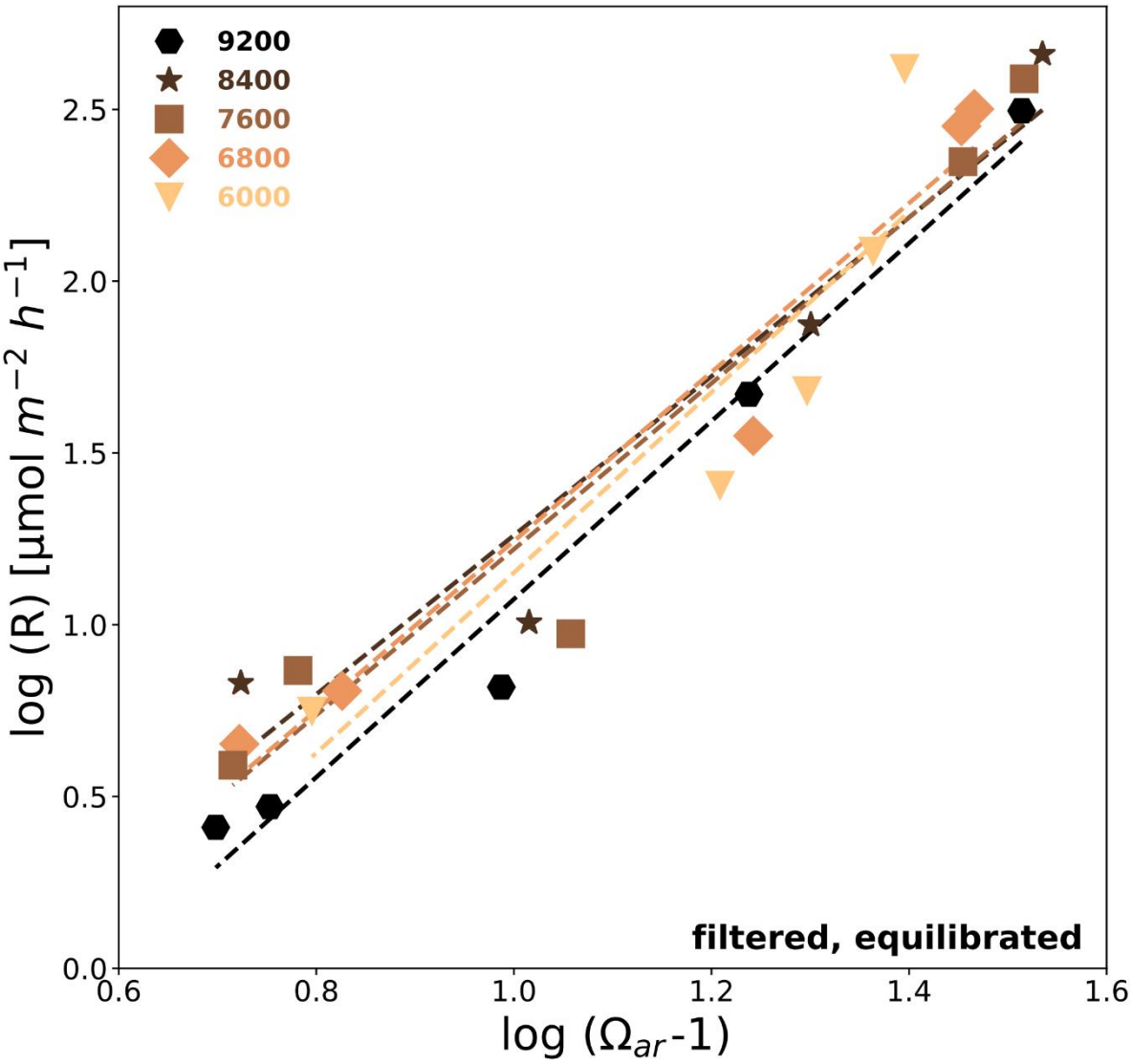

Figure S9: Carbonate precipitation kinetics for filtered eq treatments that entered the APP; see Tab. S7 for related regressions and rate equations.

Table S7: Overview of coefficients and regressions of empirical rate equations for filtered eq treatments, also see Fig. S9 and Tab. S8.

Treatment	$\log(R) = n(\Omega_{ar} - 1) + \log(k)$			
ΔTA	n	log(k)	R^2	$\hat{\sigma}$
9200	2.59	-1.52	0.823	0.118
8400	2.31	-1.05	0.963	0.078
7600	2.41	-1.19	0.942	0.103
6800	2.46	-1.22	0.925	0.118
6000	2.63	-1.47	0.977	0.060
all	2.49	-1.31	0.931	0.214

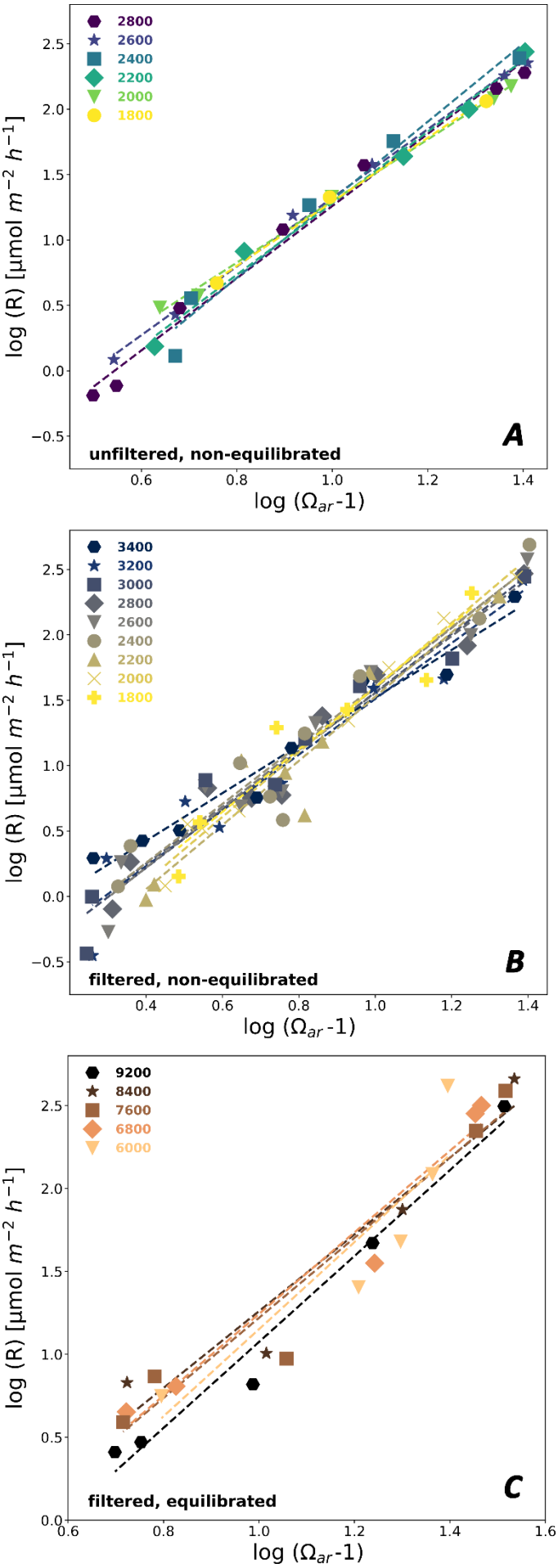

Figure S10: Comparison carbonate precipitation kinetics. (A) unfiltered, neq (B) filtered neq, (C) filtered eq treatments. Original plots shown in Fig. 6, S8 and S9.

Table *S8: Overview of all determined reaction orders (n), rate constants (k) and curve fit coefficients (a, b, c, d) for cross-comparison.*

Treatment		$\log(R) = n(\Omega_{ar} - 1) + \log(k)$		$f(t) = a\, e^{-be^{-ct}}$			
	ΔTA	n	log(k)	a	b	c	d
unfiltered non-CO_2-equilibrated	**2800**	2.76	-1.50	-3162.94	5.88	0.64	4426.60
	2600	2.62	-1.30	-3184.57	6.66	0.66	4458.90
	2400	2.98	-1.68	-3162.95	5.09	0.65	4466.20
	2200	2.73	-1.45	-3091.21	5.22	0.38	4292.50
	2000	2.35	-1.06	-2841.46	24.49	0.40	4106.00
	1800	2.45	-1.16	-2503.10	86.03	0.35	3924.60
	1600	-	-	-1932.75	-252.65	-0.30	3686.50
filtered non-CO_2-equilibrated	**3400**	1.82	-0.30	-3359.0	4.55	0.87	4460.4
	3200	2.13	-0.62	-3368.1	5.76	1.08	4511.3
	3000	2.24	-0.68	-3312.2	5.94	1.01	4437.7
	2800	2.18	-0.62	-3294.8	4.59	0.80	4497.5
	2600	2.29	-0.70	-3333.5	5.17	0.84	4506.1
	2400	2.25	-0.64	-3238.0	6.51	0.91	4426.4
	2200	2.45	-0.93	-3121.7	8.06	0.86	4294.1
	2000	2.47	-0.88	-2976.7	8.75	0.59	4090.1
	1800	2.38	-0.78	-2753.5	16.77	0.49	3943.1
filtered CO_2-equilibrated	**9200**	2.59	-1.52	-3957.4	4.73	1.23	11202.3
	8400	2.31	-1.05	-3522.1	7.65	1.26	10387.4
	7600	2.41	-1.19	-3017.7	10.63	0.87	9646.6
	6800	2.46	-1.22	-2583.1	11.99	0.69	8829.9
	6000	2.63	-1.47	-2499.5	5.50	0.33	8058.7
	5200	-	-	-1401.0	121.95	0.36	7273.7

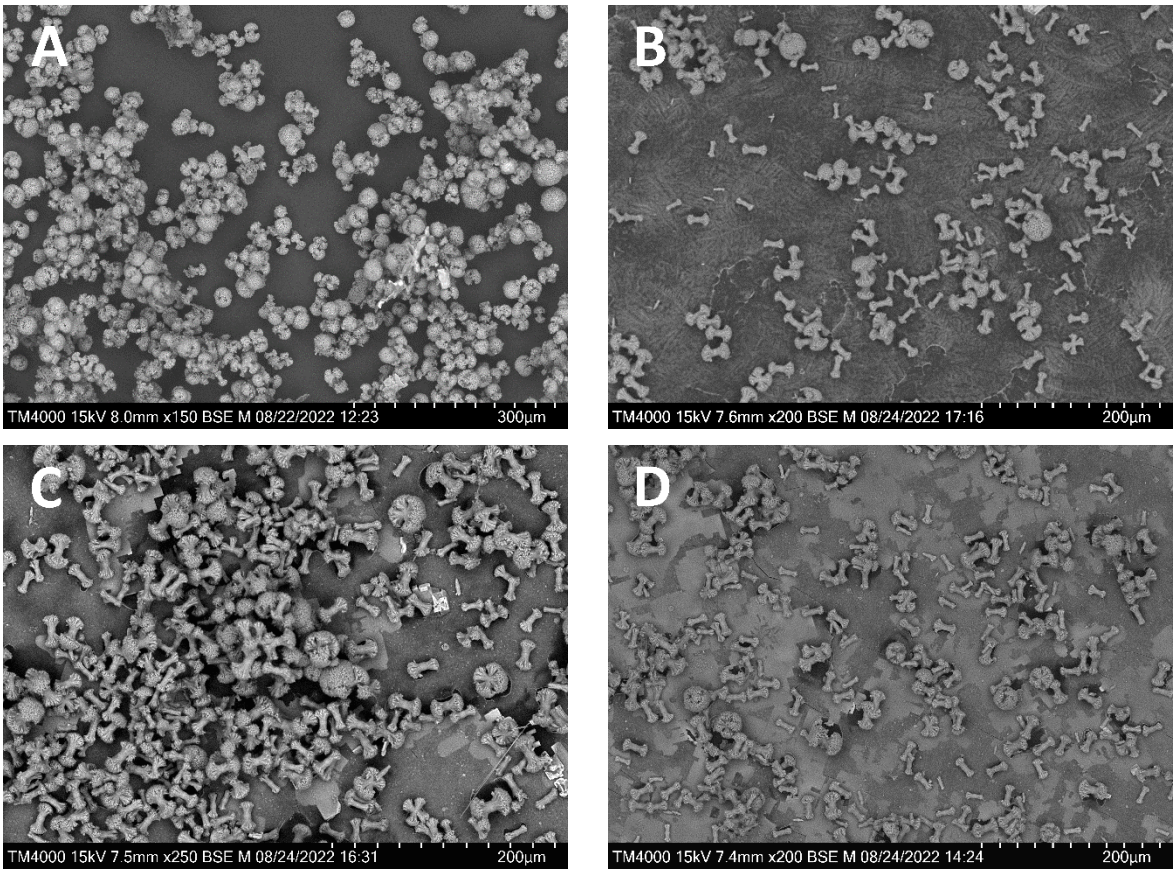

Figure S11: SEM images to determine size distributions, (A) neq filtered ΔTA_{2400} *Gran Canaria; (B) neq unfiltered* ΔTA_{2600} *Raunefjorden, Bergen; (C) and (D) neq unfiltered* ΔTA_{2800} *– Raunefjorden, Bergen.*

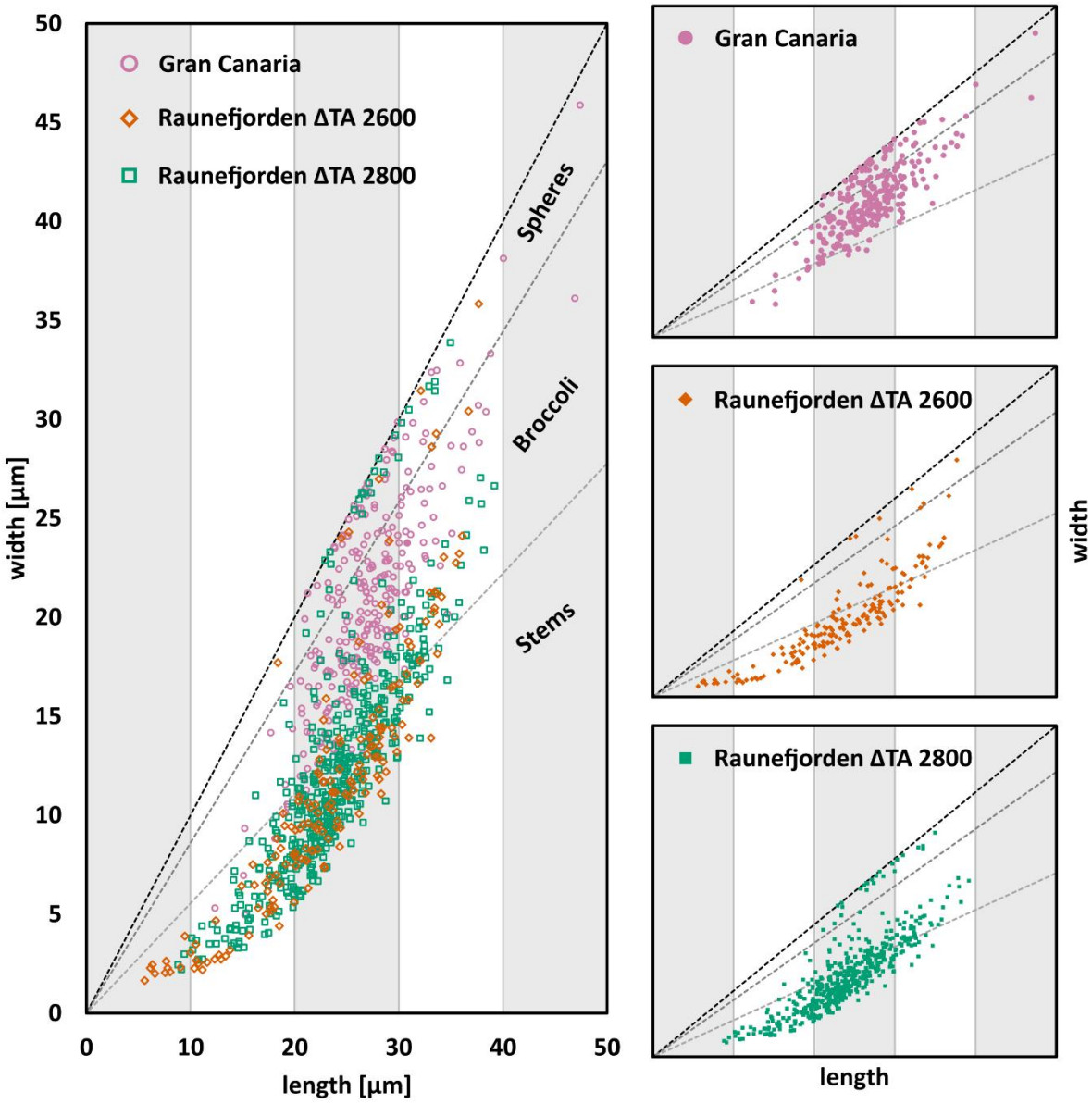

Figure S12: Sizes of precipitated particles during incubation experiments on Gran Canaria (pink circles) (see Hartmann et al., 2023) and in the Raunefjorden, Bergen (see Suitner et al., 2024). Bergen data showcase particles from incubation experiments increasing TA by 2600 (orange diamonds) and 2800 µmol kg^{-1} (green squares); particles were manually counted via SEM images and categorized in three types (spheres, "broccoli" (see Morse et al., 2007 and Suitner et al., 2024), and stems). For a categorization width:length ratios are indicated by dotted lines, sphere (width:length >0.9) – broccoli (width:length 0.5>x>0.9) – stems (width:length >0.5). See Fig. S11 for original SEM images.

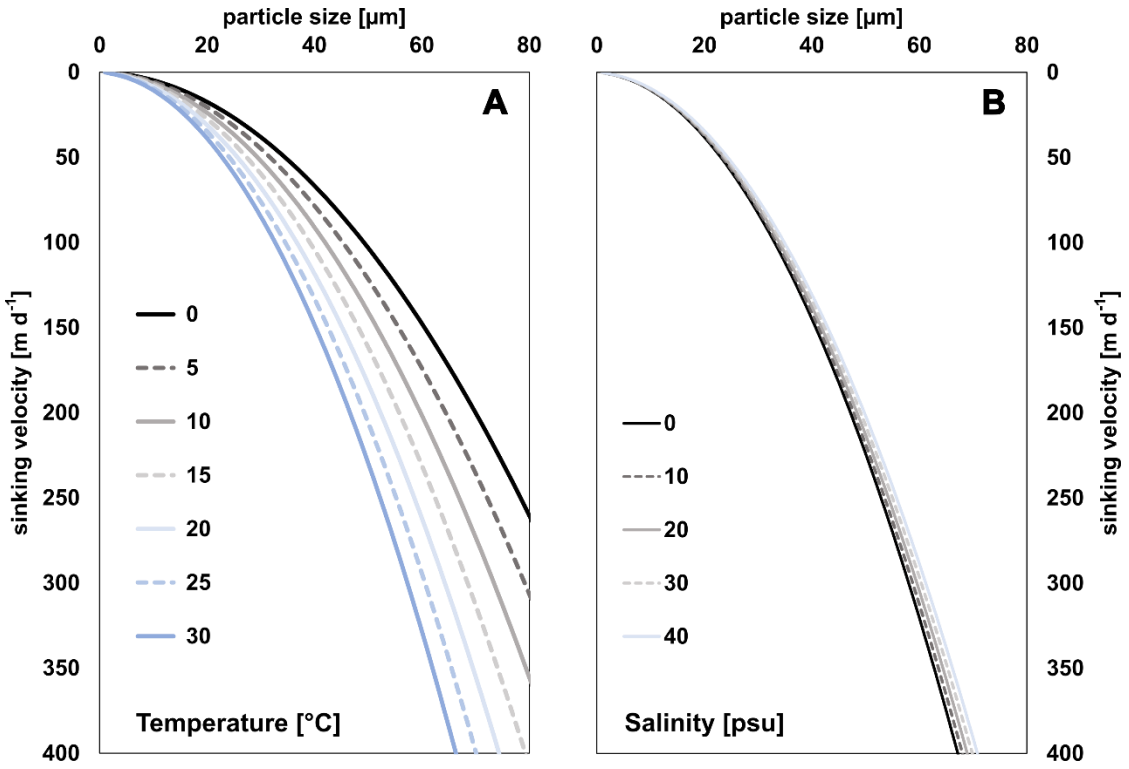

Figure S13: (A) Influence of temperature (salinity fixed to 35 psu) and (B) salinity (temperature fixed to 10°C) variations on sinking velocity.

111

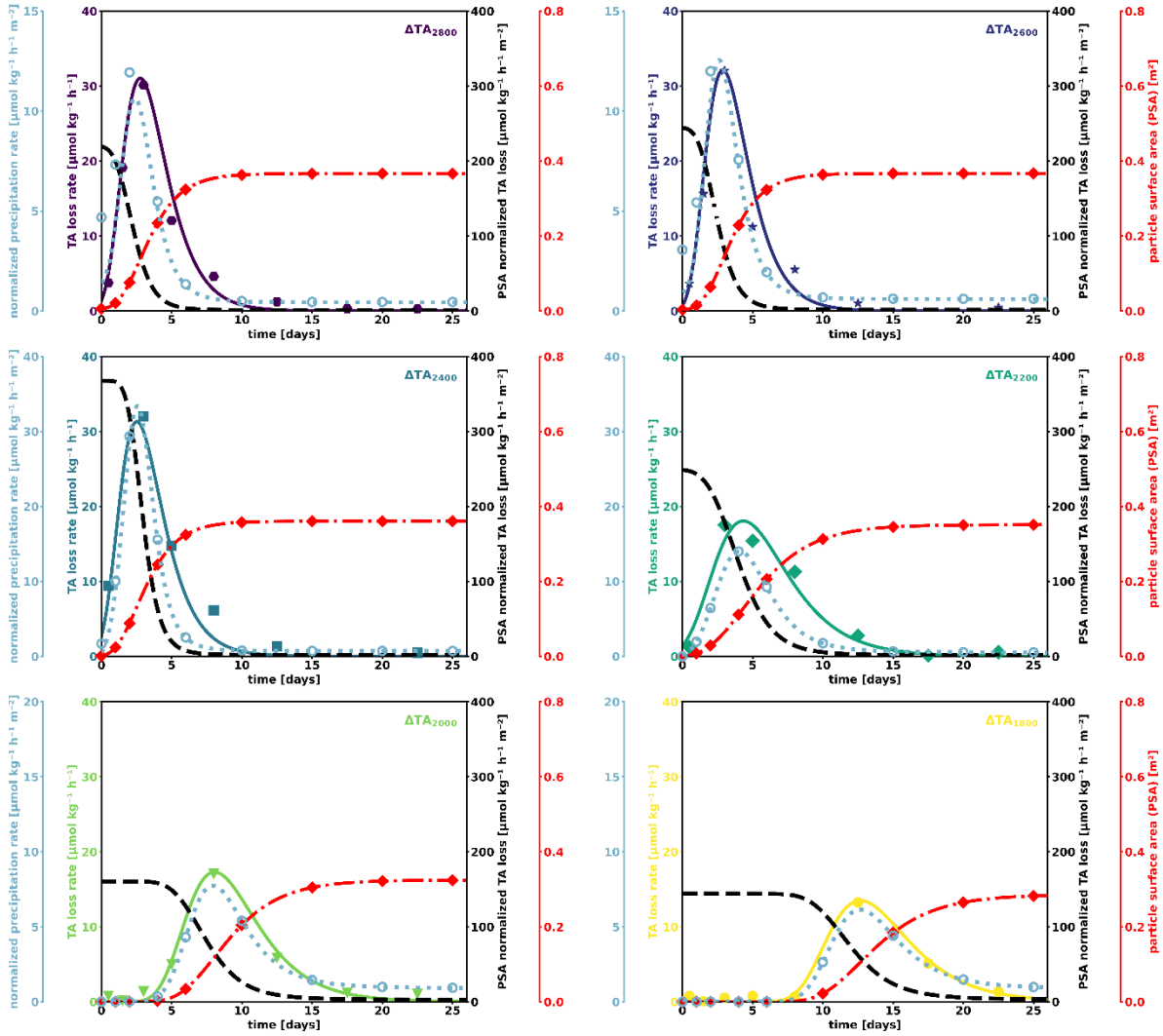

Figure S14: Conceptual figures, showcasing the interplay of Ω_{ar} and particle surface area guiding the theoretical TA-loss rate evolution (dashed lines) in the unfiltered non-CO_2-equilibrated treatments (Raunefjorden); particle surface area (dash-dotted, red); curve fitted TA-loss rate (solid lines), measured TA-loss rates are represented by markers of matching colors. Light blue dotted lines: empirical rate equations, including determined rate constants (k) and reaction orders (n), expected precipitation rate and particle surface area (also see Fig. 8 and related text). Hollow light-blue markers provide the output of the related empirical rate equations for each sampling day (also see Tab. 3). Please note that the scales of the normalized precipitation rate (light blue) are not consistent across all plots.

112

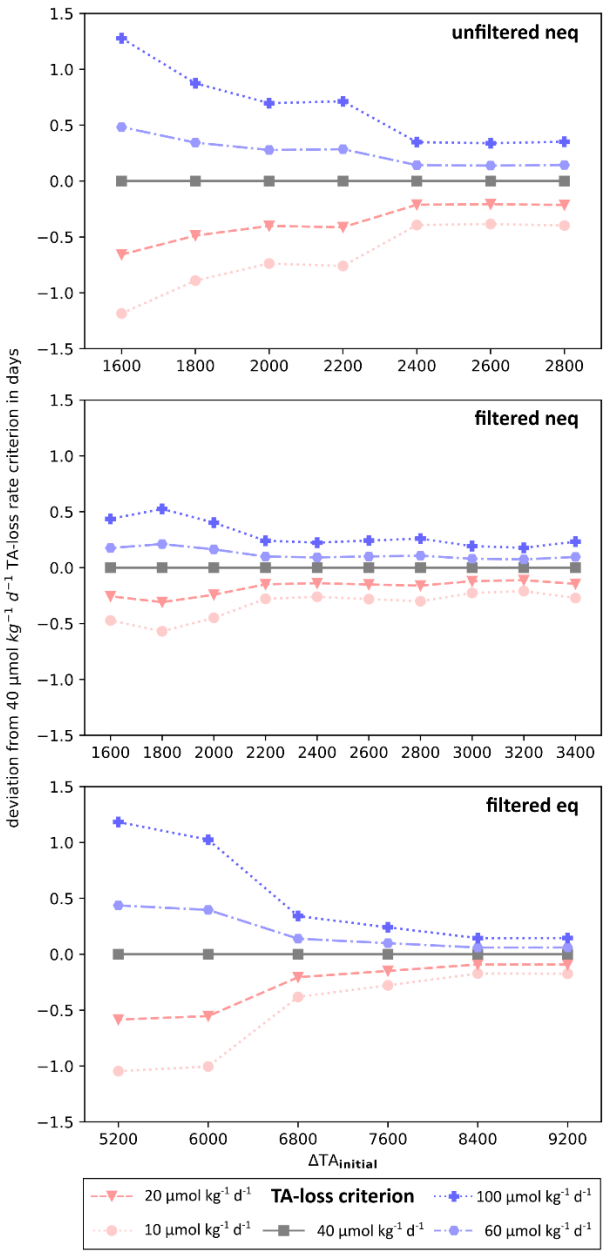

Figure S15: Deviation of onset of the APP with varying TA-loss criteria (see legend) for the unfiltered neq (A), filtered neq (B), and filtered eq (C) experiments.

113

Conceptual framework to analyze surface area loss during sinking

To estimate the reduction in surface area resulting from the settling of precipitated particles from an assumed alkalized plume of 10 meters, discrete particle diameter size classes were set in increments of 5 µm: specifically, 0-5 µm, 5-10 µm, 10-15 µm, 15-20 µm, 20-25 µm, 25-30 µm, and 30-35 µm. These size classes are based on the distinct particle classifications outlined in section 3.6 and in the study by Suitner et al. (2024). With the known size distributions and aragonite formation rates, treatment level ΔTA_{2800} from the unfiltered non-CO_2-equilibrated experiment (Raunefjorden) was employed as an analogous example to demonstrate the concept of the surface area reduction resulting from particle sinking.

To simplify the calculations, particles were assumed to be spheres with equivalent spherical diameters (ESD) corresponding to the specified size classes. Particles were allowed to transition to the next larger size class in increments of 4 hours, following constant transition factors. Derived from the curve-fitted TA-loss rates, the mass of precipitated aragonite particles is known. When combined with the known size class distribution after 6 days, transition factors and particle counts for each size class can be calculated (see Fig. S10). By assuming uniform sinking velocities for each discrete size class and applying the calculation method outlined in section 3.6, the distance traveled during the sinking process can be calculated for all possible combinations of size class transitions. Based on a set particle surface area of 2.283 $m^2\ g^{-1}$ (see section 2.3), the decrease in available surface area for heterogeneous precipitation can therefore be estimated. Since the available surface area is proportional to the precipitation rate (Eq. 4), the settling of precipitated particles would delay or even stop the precipitation process. Assuming a 10 m alkalized layer, the present example suggests that the available surface area would be reduced by ~35 %, if an export mechanism is incorporated in the treatment level ΔTA_{2800} from the unfiltered non-CO_2-equilibrated experiment.

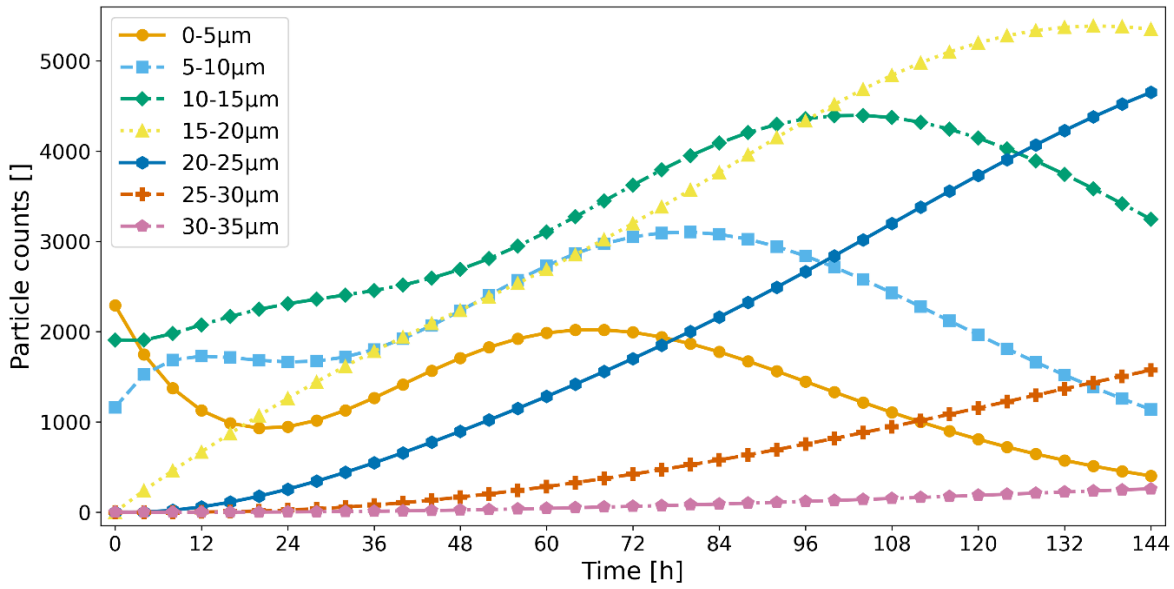

Figure S16: Temporal evolution of particle counts for each designated size class; see text above for details on the calculations and methodology used.